Ab initio no-core full configuration calculations of light nuclei

P. Maris,[1] J. P. Vary,[1] and A. M. Shirokov[1,2]
[1]*Department of Physics and Astronomy, Iowa State University, Ames, Iowa 50011, USA*
[2]*Skobeltsyn Institute of Nuclear Physics, Moscow State University, RU-119991 Moscow, Russia*
(Received 28 August 2008; published 22 January 2009)

We perform no-core full configuration calculations for a set of light nuclei including ^{16}O with a realistic NN interaction, JISP16. We obtain ground-state energies and their uncertainties through exponential extrapolations that we demonstrate are reliable in ^{2}H, ^{3}H, and ^{4}He test cases where fully converged results are obtained directly. We find that ^{6}He, ^{6}Li, and ^{8}He are underbound by about 600 keV, 560 keV, and 1.7 MeV, respectively. ^{12}C is overbound by about 1.7 MeV and ^{16}O is overbound by about 16 MeV. The first excited 0^+ states in ^{12}C and ^{16}O are also evaluated but their uncertainties are significantly larger than the uncertainties for the ground states.

DOI: 10.1103/PhysRevC.79.014308 PACS number(s): 21.60.De, 21.60.Cs, 21.45.−v, 21.30.−x

I. INTRODUCTION AND MOTIVATION

The rapid development of *ab initio* methods for solving finite nuclei has opened a range of nuclear phenomena that can be evaluated to high precision using realistic nucleon-nucleon (NN) and three-nucleon (NNN) interactions. Such advances define a path for testing fundamental properties of the strong interaction such as their origins from QCD via chiral effective field theory [1–4]. In addition, they prepare a foundation for nuclear reaction theory with unprecedented predictive power.

Here we investigate the direct solution of the nuclear many-body problem by diagonalization in a sufficiently large basis space that converged binding energies are accessed—either directly or by simple extrapolation. Our choice is a traditional harmonic oscillator (HO) basis so there are two basis space parameters, the HO energy $\hbar\Omega$ and the many-body basis space cutoff $N_{\max}$. $N_{\max}$ is defined as the maximum number of total oscillator quanta allowed in the many-body basis space above the minimum for that nucleus. We obtain convergence in this two-dimensional parameter space ($\hbar\Omega$, $N_{\max}$), where convergence is defined as independence of both parameters within evaluated uncertainties.

Because we treat all nucleons equivalently and we achieve convergence within evaluated uncertainties, we refer to our approach as the no-core full configuration (NCFC) method. The NCFC is both related to and distinct from the no-core shell model (NCSM) [5] that features a finite matrix truncation and an effective Hamiltonian renormalized to that finite space. The regulator, $N_{\max}$, appears in our NCFC, where it is taken to infinity, and in the NCSM, where it also appears in the definition of the effective Hamiltonian. In both NCFC and NCSM, this choice of many-body basis regulator, $N_{\max}$, is needed to preserve Galilean invariance—to factorize all solutions into a product of intrinsic and center-of-mass motion components. With $N_{\max}$ as the regulator, both the NCFC and the NCSM are distinguished from the full configuration interaction (FCI) method in atomic and molecular physics that employs a cutoff in single-particle space.

The NCFC results should agree with the NCSM and no-core FCI results when the latter results are obtained in sufficiently large basis spaces. In the case of NCSM, larger cluster sizes for the effective Hamiltonian may be employed to accelerate convergence.

Given the rapid advances in algorithms and computers, as well as the development of realistic nonlocal NN interactions that facilitate convergence, we are able to achieve converged results, either directly or through extrapolation, without recourse to renormalization of the interaction. That is, with our adopted interaction, we do not need to soften the NN interaction by treating it with an effective interaction formalism. Renormalization formalisms necessarily generate many-body interactions that significantly complicate the calculations and are often truncated for that reason. Renormalization without retaining the effective many-body potentials abandons the variational upper bound characteristic that we prefer to retain. Furthermore, convergence with increasing model space is generally neither uniform nor monotonic when applying renormalization without retaining the induced many-body potentials. This leads to challenges for extrapolation to infinite model spaces.

Our NCFC approach requires methods to reliably extrapolate results obtained in a finite basis space to the infinite or complete basis space limit. This need for extrapolation tools mirrors similar situations in other fields of science where a sequence of results with increasing resolution must be extrapolated to the limit of infinite resolution. The resulting high-precision results of the NCFC do not agree exactly with experiment. Indeed, no known realistic NN interactions provide exact descriptions of a similar range of nuclear data that we examine and it is probable that NNN and higher-body interactions are needed.

To further motivate our efforts to develop robust extrapolation tools, we show in Fig. 1 the Hamiltonian matrix dimensions for a set of representative light nuclei. We employ the "m-scheme" where each HO single-particle state has its orbital and spin angular momenta coupled to good total angular momentum, j, and magnetic projection, m. The many-body basis states are Slater determinants in this HO basis and are limited by the imposed symmetries—parity and total angular momentum projection (M), as well as by $N_{\max}$. In the natural-parity cases for even nuclei shown, $M = 0$ enables the simultaneous calculation of the entire spectrum for that parity and $N_{\max}$.

The nearly exponential growth in matrix dimension with increasing $N_{\max}$ is clearly evident in Fig. 1. To achieve

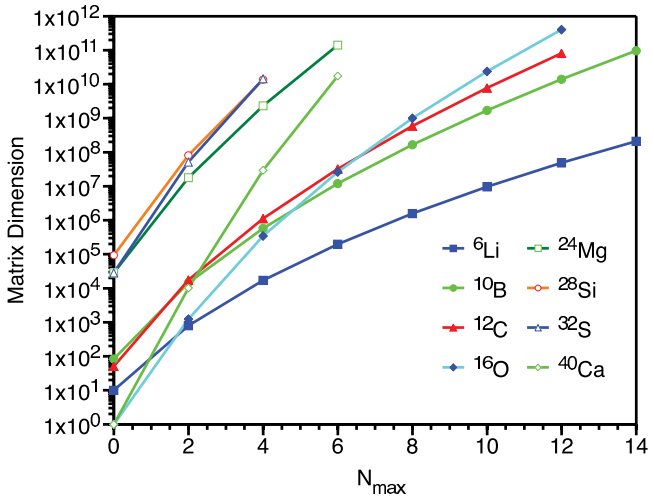

FIG. 1. (Color online) Representative Hamiltonian matrix dimensions for total magnetic projection $M = 0$ states in the single-particle m-scheme as a function of the maximum total oscillator quanta of excitations specified by $N_{\max}$. The natural-parity matrix dimensions are represented by the specific points while unnatural-parity matrix dimensions would lie close to the interpolating lines at odd values of $N_{\max}$.

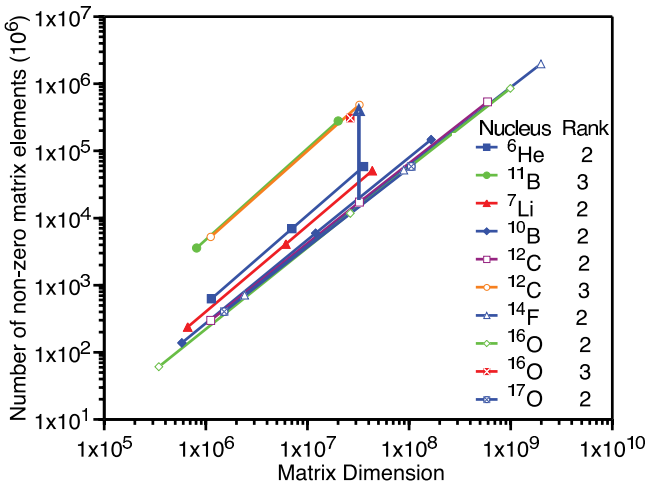

FIG. 2. (Color online) Number of nonvanishing many-body Hamiltonian matrix elements for representative light nuclei as a function of the basis space dimension. The points represent sample cases that have been solved and correspond to those indicated in the legend. The curves approximate a $D^{3/2}$ power law where D is the basis space dimension. The vertical arrow measures a factor of 30 between the two-body Hamiltonian (rank = 2) and three-body Hamiltonian (rank = 3) cases for ^{12}C at the same dimension corresponding to $N_{\max} = 6$. Note the logarithmic scales.

NCFC results for the heavier of these nuclei by extrapolation, using realistic interactions, we would need to diagonalize matrices that are beyond the reach of present technologies. However, in cases up to and including ^{16}O, we may expect to obtain systematic results for the first few increments of $N_{\max}$. To use the sequence of results obtained with $N_{\max}$ values that are currently accessible, we need to investigate suitable extrapolation tools.

To better understand the scale of computational effort needed for no-core microscopic nuclear structure studies, we consider the memory storage demands as a function of matrix dimension. For several representative nuclei, we enumerate the number of nonvanishing matrix elements of the resulting many-body Hamiltonian matrix (its lower triangle only for efficiency) and display the resulting counts as a function of the matrix dimension in Fig. 2. We present results for the case of a two-body input Hamiltonian (NN interaction only) and for the case of a three-body Hamiltonian ($NN + NNN$ interactions). In spite of the very large memory requirements, the various curves display an encouraging trend. Specifically, the number of nonvanishing many-body matrix elements follows a $D^{3/2}$ growth rate, where D is the dimension of the matrix. That is, the matrices exhibit a very sparse character and this is the property that allows us to diagonalize the large matrices that we can presently solve.

II. SELECTION OF HAMILTONIAN INGREDIENTS AND EXAMPLE NUCLEI

To carry out the NCFC calculations, we require a realistic NN interaction that is sufficiently weak at high-momentum transfers that we can obtain a reasonable convergence trend. The conventional Lee-Suzuki-Okamoto renormalization procedure of the *ab initio* NCSM [5] develops soft, $N_{\max}$-dependent, effective interactions that provide answers close to experimental observations. However, the convergence trend of the results with increasing $N_{\max}$ is often not uniform and leads to challenges for extrapolation to infinite model spaces. Nevertheless, there is also encouraging progress in extrapolating NCSM ground-state energies of light nuclei using different strategies [6,7]. Of course, as the basis space increases, one expects the NCSM and NCFC methods to arrive at the same exact result. Thus, the choice of method, NCSM or NCFC, will ultimately depend on the underlying Hamiltonian selected for the application. In the NCFC approach discussed here, we seek to obtain the ground-state energy of the original, or "bare" [8], Hamiltonian in the infinite model space with evaluated uncertainties. To this end, we incorporate systematic and reliable extrapolation tools as needed.

We compare in Fig. 3 the ground state of ^{4}He using the next-to-next-to-next-to leading-order (N3LO) chiral interaction, [3,9], with the ground-state energy using the J-matrix inverse scattering potential (JISP16) [10,11] and plotted as a function of $N_{\max}$ to ascertain convergence rates. All our results include the Coulomb interaction between protons. Each point represents the ground-state energy from an $N_{\max}$ truncation of the full infinite matrix problem. Hence, all points are strict upper bounds on the exact ground-state energies for the respective Hamiltonian. Figure 3 shows that JISP16 provides a faster convergence rate and a ground-state energy in closer agreement with the experimental energy of -28.296 MeV. JISP16 also produces spectra and other observables in light nuclei that are in reasonable accord with experiment [10]. Indeed, this interaction was designed to possess these specific properties while retaining an excellent description of the NN

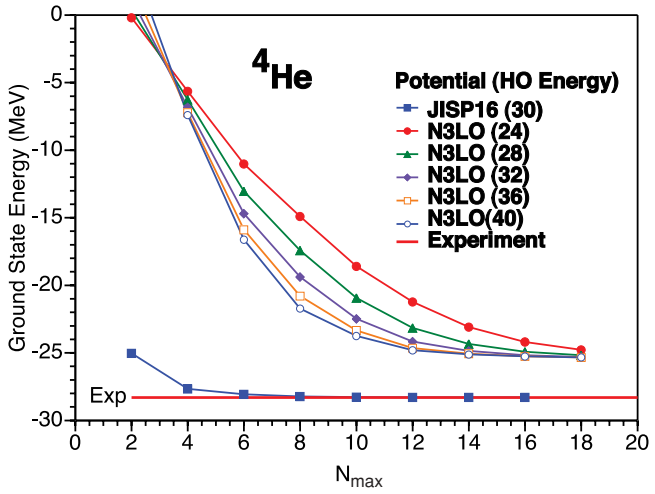

FIG. 3. (Color online) Calculated ground-state energy of ^{4}He as a function of $N_{\max}$ at various values of the oscillator energy, $\hbar\Omega$, as indicated in the legend. The results are connected by straight-line segments to guide the eye. The results with chiral N3LO are from Ref. [9]. The results for JISP16 are closer to convergence even in rather modest basis spaces. No extrapolations are needed in these cases as converged results are obtained directly.

data. The interaction is nonlocal but this is no limitation for NCFC, which also preserves all the symmetries of the underlying NN interaction.

With JISP16 for our NN interaction, we perform *ab initio* calculations of the ground-state energies of ^{2}H, ^{3}H, ^{4}He, ^{6}He, ^{6}Li, ^{8}He, ^{12}C, and ^{16}O. The three lightest nuclei serve as test cases to demonstrate that the extrapolation methods, using results in limited basis spaces, are able to predict the fully converged results and to demonstrate that our assessed uncertainties are realistic. We limit ourselves to examples for which a sufficient set of results could be achieved within our current computational resource limits.

III. FINITE BASIS SPACE EXPANSIONS

Our results in finite basis spaces satisfy the variational principle and show uniform and monotonic convergence from above to the exact eigenenergy with increasing $N_{\max}$. That is, the results for the energy of the lowest state of each spin and parity, at any $N_{\max}$ truncation, are upper bounds on the exact converged answers and the convergence is monotonic with increasing $N_{\max}$. This guarantee of monotonic convergence from above to the exact energy facilitates our choice of extrapolating function.

We carefully investigate the dependence of the results on the basis space parameters, $N_{\max}$ and $\hbar\Omega$. Our goal is to achieve independence of both of these parameters as that is a signal for convergence—the result that would be obtained from solving the same problem in a complete basis.

Before proceeding, let us explain some additional features of the many-body regulator, $N_{\max}$. As introduced above, $N_{\max}$ is the maximum number of oscillator quanta shared by all nucleons above the lowest HO configuration for the chosen nucleus. Its use allows us to factorize eigenfunctions into intrinsic and center-of-mass (c.m.) components for ease of eliminating spurious center-of-mass motion effects on all observables. One unit of oscillator quanta is one unit of the quantity $(2n + l)$, where n is the principle quantum number and l is the angular quantum number. If the highest HO single-particle state of this lowest HO configuration has N_0 HO quanta, then $N_{\max} + N_0$ identifies the highest HO single-particle states that can be occupied within this many-body basis. Note that because $N_{\max}$ is the maximum of the *total* HO quanta above the minimal HO configuration, we can have at most one nucleon in such a highest HO single-particle state.

The precise method of achieving the factorization of the center-of-mass and intrinsic components of the many-body wave function follows a standard approach, sometimes referred to as the Lawson method [12]. In this method, one selects the many-body basis space in the manner described above and adds a Lagrange multiplier term to the many-body Hamiltonian $\lambda(H_{\text{c.m.}} - \frac{3}{2}\hbar\Omega)$, where $H_{\text{c.m.}}$ is the harmonic oscillator Hamiltonian for the center-of-mass motion. With λ chosen positive (10 is a typical value), one separates the states of lowest center-of-mass motion $(0S_{\frac{1}{2}})$ from the states with excited center-of-mass motion by a scale of order $\lambda\hbar\Omega$. The resulting low-lying states have wave functions that are assured to have the desired factorized form.

It is important to note that our NCFC results for the ground-state energy for $A = 2, 3, 4$ are obtained directly as we achieve sufficient independence of $N_{\max}$ and $\hbar\Omega$. For the other nuclei studied here, we characterize the approach to convergence by the dependence of results on both $N_{\max}$ and $\hbar\Omega$ and investigate the shape of that convergence in detail. The degree of residual dependence on these two parameters provides a measure of the difference from the exact result, an estimate of the numerical uncertainty in the extrapolation.

We employ the parallel-processor code MANY-FERMION DYNAMICS–NUCLEAR (MFDn) [13] that sets up the many-body basis space, evaluates the many-body Hamiltonian matrix, obtains the low-lying eigenvalues and eigenvectors using the Lanczos algorithm, and evaluates a suite of experimental observables. Working in the single-particle HO m-scheme, the lowest 15 states here are usually obtained with 300–600 iterations, depending on $N_{\max}$ and the nucleus involved. The required number of iterations grows with $N_{\max}$.

The largest matrix we diagonalize for this work corresponds to ^{16}O in the $N_{\max} = 8$ space with a basis dimension about 1 billion. We obtain the lowest 8 eigenstates and a suite of observables in 4.5 hours on 12,090 processors using the Franklin supercomputer at the National Energy Research Supercomputer Center (NERSC). The second largest case is ^{12}C with a basis dimension of about 600 million for which we obtain the lowest 15 eigenstates and a suite of observables in 2.3 hours on 12,720 processors using the Jaguar supercomputer at Oak Ridge National Laboratory (ORNL). The above times correspond to calculations at a single value of $\hbar\Omega$. For calculations as a function of $\hbar\Omega$ in the same basis spaces, we use internally generated and stored index arrays amounting to many terabytes of data so that the second and subsequent $\hbar\Omega$ values each take about 2/3 the time of the first case.

Following the completion of the calculations reported here, further speedups have been accomplished with the code so that the above-mentioned times are reduced by a factor of 2 in future calculations of the same type [14].

IV. EXTRAPOLATING THE GROUND-STATE ENERGY

A. Simple illustration

Here we illustrate the convergence properties for the nuclear ground-state energy in a HO basis with a simple model. Although the properties of the HO basis are useful for many purposes, such as the exact treatment of the center-of-mass motion and the ease of transforming between relative and single-particle coordinates, the asymptotic HO wave functions are Gaussians while wave functions of finite nuclei will have exponentially decreasing amplitudes at large distances. Correct long-range behavior is important for precision evaluation of energies and for many other experimental properties such as electromagnetic moments and transition rates. To achieve converged long-range observables, we expect to require an optimal choice of the $\hbar\Omega$ value and sufficiently large values of $N_{\max}$ to generate good asymptotic properties. To investigate these issues, we evaluate the properties of fermions in a finite phenomenological potential, the picture that underlies the successful nuclear shell model, using a HO basis expansion.

Consider the properties of a single Slater determinant composed of the lowest A-particle orbits of the Saxon-Woods central potential plus a nuclear spin-orbit potential. This corresponds to a standard mean-field description of the nucleus with A nucleons and we refer to this simple model as the extreme single-particle model (ESPM). Instead of solving for the single-particle states by numerical integration, we diagonalize the one-body model Hamiltonian in a HO basis to simulate the procedures of a no-core finite HO basis calculation.

We adopt ^{12}C as an example and we perform this diagonalization as a function of $N_{\max}$ and $\hbar\Omega$. In this way, we are studying how the lowest s-state and p-state solutions depend on $N_{\max}$ and $\hbar\Omega$. We identify $N_{\max}$ with the maximum value of the HO quanta $(2n + l)$ retained in the HO basis expansion so that $N_{\max} = 0$ corresponds to a pure HO approximation, $N_{\max} = 2$ employs two basis HO functions for the occupied $0s$ states and $0p$ states, $N_{\max} = 4$ employs three basis HO functions for the occupied single-particle states, and so on. Note, there is a difference between the use of $N_{\max}$ in this model problem from our NCFC approach. Here, since we work entirely in a single-particle basis, all particles have simultaneous access to the range of basis states dictated by $N_{\max}$ while in our NCFC, the many-body basis is restricted so that as one particle takes more quanta, the remaining particles take fewer quanta.

It should be noted that our model problem more closely simulates the traditional FCI approach used in quantum chemistry where orbits are equally accessible in the many-body basis states up to some single-particle cutoff. The origin of this difference is our need to retain an exact treatment of the center-of-mass motion in our no-core methods for finite nuclei (NCFC and NCSM). In spite of this difference in cutoffs, we find that this simple model is useful for illustrating how proper asymptotic wave function properties influence convergence rates for self-bound nuclei in the HO basis.

We adopt Saxon-Woods central, $U(r)$, and spin-orbit, $U_{\rm so}(r)$, potentials similar to a standard choice [15] where, for simplicity, we use the same parameters for the neutrons and the protons of ^{12}C

$$U(r) = \frac{U_0}{1 + \exp[(r - R)/a_0]}$$

$$U_{\rm so}(r) = \mathbf{S}\cdot\mathbf{L}\left(\frac{\hbar}{m_\pi c^2}\right)^2 \frac{1}{r}\frac{d}{dr}\frac{U_{\rm so}}{1 + \exp[(r - R)/a_{\rm so}]},$$

with $R = r_0 A^{1/3}$ and $(\frac{\hbar}{m_\pi c^2})^2 = 2.0$ fm^2. Our parameters selected for this demonstration are $U_0 = -32$ MeV, $r_0 = 1.25$ fm, $a_0 = 0.65$ fm, $U_{\rm so} = 15$ MeV and $a_{\rm so} = 0.47$ fm. For the protons we add the Coulomb field of a uniformly charged sphere of radius R.

We add the energies of the occupied orbits, taking into account degeneracies, to obtain the total energy of the system in the ESPM. The resulting ESPM ground-state energy for ^{12}C is displayed in Fig. 4 as a function of $\hbar\Omega$ for a range of $N_{\max}$ values up to and including $N_{\max} = 20$. The line segments connect the results calculated at selected values of $\hbar\Omega$. Here we observe a pattern that is typical of our no-core basis space results presented below—a sequence of curves with energy decreasing as a function of increasing $N_{\max}$, consistent with the property dictated by the variational principle. With increasing $N_{\max}$, one approaches convergence signaled by achieving simultaneous independence of both $N_{\max}$ and $\hbar\Omega$. In the ESPM, we achieve the total energy converged to within 10 keV at $N_{\max} = 20$ over the range $\hbar\Omega = 6-11$ MeV. For the optimal value of $\hbar\Omega = 7$ MeV, we achieve a total energy to within 170 keV of the

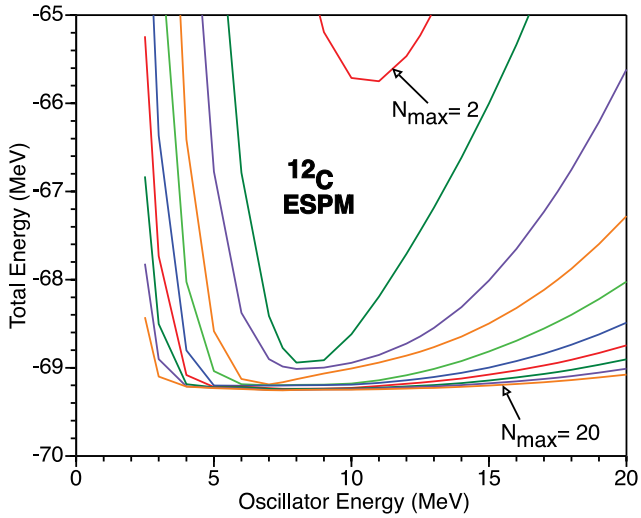

FIG. 4. (Color online) Calculated ground-state energy of ^{12}C in the ESPM as a function of $\hbar\Omega$ and $N_{\max}$, the maximum value of the HO states' quanta, $2n + l$, used in expanding the Saxon-Woods single-particle states. The curve closest to convergence corresponds to the value $N_{\max} = 20$ and successively higher curves are obtained with $N_{\max}$ decreased by 2 units for each curve.

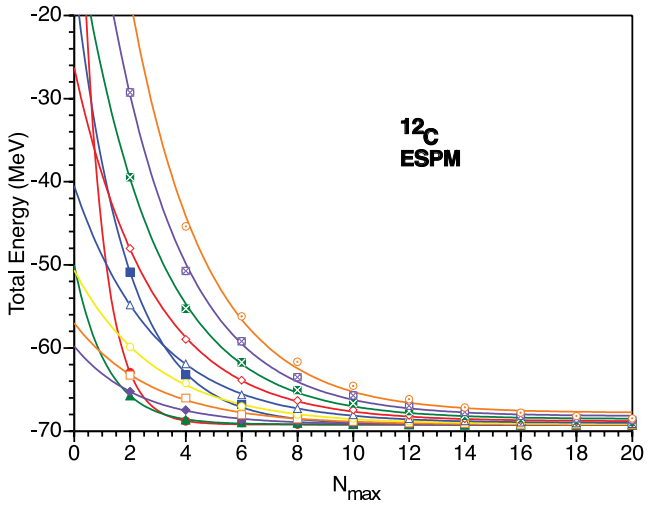

FIG. 5. (Color online) Calculated ground-state energy of ^{12}C in the ESPM as a function of $N_{\max}$ for selected values of $\hbar\Omega$ used in defining the basis states. The points correspond to $\hbar\Omega$ values ranging from 5 to 30 MeV in 2.5-MeV increments. The curves represent an exponential plus a constant fit to each set of results at fixed $\hbar\Omega$, excluding the $N_{\max} = 0$ result. Each point carries equal weight.

exact answer already at $N_{\max} = 8$, yielding an upper bound within 0.25% of the exact result.

For the purpose of exploring potential extrapolation tools, we use the results of the ESPM to map out the convergence pattern of the total energy in the present work. In subsequent efforts, we will investigate other observables in a similar fashion. Thus, we present in Fig. 5 the total energy as a function of $N_{\max}$ at fixed values of $\hbar\Omega$ spanning the minima of the curves in Fig. 4. Specifically, the points correspond to $\hbar\Omega$ values ranging from 5 to 30 MeV in 2.5-MeV increments. We find that, once we exclude the $N_{\max} = 0$ result, the calculated points appear to represent an exponential convergence pattern. To confirm this, we fit an exponential plus constant to each set of results as a function of $N_{\max}$, excluding $N_{\max} = 0$, and the resulting fits are displayed in Fig. 5 as smooth curves. That is, for each set of points at fixed $\hbar\Omega$, we fit the ground-state energy with three adjustable parameters using the relation

$$E_{\rm gs}(N_{\max}) = a \exp(-c\, N_{\max}) + E_{\rm gs}(\infty). \qquad (1)$$

In these fits, we assign equal weight to each point and perform a regression analysis.

Overall, we conclude that the exponential plus constant fits the results rather well. Thus, one observes that the HO basis provides a rapidly converging sequence of total energies in the ESPM, one well-represented by exponential convergence in $N_{\max}$ toward the the asymptotic total energy, $E_{\rm gs}(\infty)$. It appears reasonable to expect this convergence pattern of the HO basis treatment of the ESPM to be representative of HO basis expansion behavior in our no-core applications, we will adopt this functional form as a foundation for further developing our extrapolation methods below. In the following sections, we will use additional arguments to improve on this tool and test it in light nuclei where converged results are obtained directly.

We note that a similar exponential behavior for HO basis space calculations of a cold trapped Fermi gas has been observed [16]. In that case, the same type of single-particle-space regulator was employed as we use here in the ESPM application.

The exponential plus constant was also employed as an extrapolation tool in more conventional shell-model studies [17]. In those applications, the variable is the matrix dimension rather than $N_{\max}$.

B. NCFC test case: deuteron

Next, we turn to the NCFC calculations for light nuclei using JISP16, where we can achieve nearly exact results in large model spaces. In this and the following subsections, we investigate the convergence rates for the ground-state energies as a function of $N_{\max}$ and $\hbar\Omega$ for ^{2}H, ^{3}H, and ^{4}He. We discuss two extrapolation methods, which allow us to obtain estimates of the converged NCFC results from finite model spaces. We also introduce the assessed uncertainties for our extrapolated results.

The sequence of curves in Fig. 6 for ^{2}H illustrates the trends we encounter in our calculations when evaluating the ground-state energy with JISP16. Our purpose with ^{2}H is only to illustrate convergence trends and test the extrapolation tool because the exact answer is also available from the direct solution of the Schroedinger equation [18] and agrees with experiment. The $N_{\max} = 18$ curve reaches to within 9 keV of this exact result; the $N_{\max} = 20$ curve reaches to within 5 keV. We note that the weak binding of ^{2}H leads to a slow progression of the curves toward independence of $\hbar\Omega$ and contrasts the stronger binding situation obtained for ^{4}He discussed below in Sec. IV C.

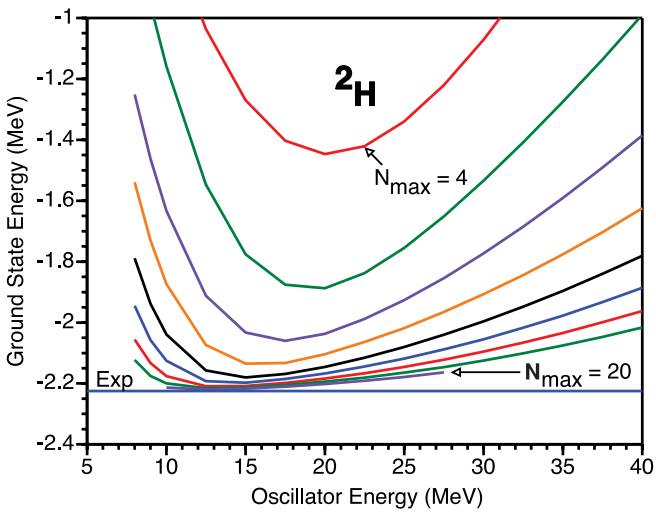

FIG. 6. (Color online) Calculated ground-state energy of ^{2}H as a function of the oscillator energy, $\hbar\Omega$, for selected values of $N_{\max}$ used in defining the basis states. The curve closest to experiment corresponds to the value $N_{\max} = 20$ and successively higher curves are obtained with $N_{\max}$ decreased by two units for each curve. The curves are formed by straight-line segments joining calculated results.

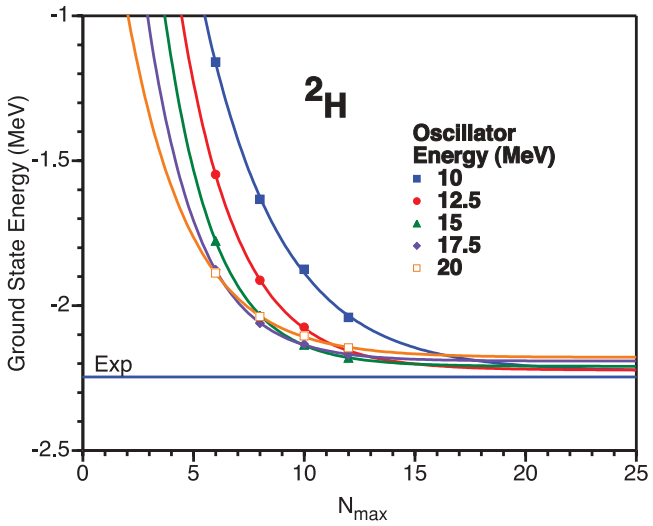

FIG. 7. (Color online) Calculated ground-state energy of ^{2}H as a function of $N_{\max}$ at $\hbar\Omega$ values that bracket the best upper bound as described in the text. The smooth curves are fits by Eq. (1) to the four data points shown at each value of $\hbar\Omega$ with each point weighted equally.

1. Global extrapolation method

We use these ^{2}H results to test our "global extrapolation method" (referred to as "extrapolation A") as illustrated in Fig. 7. Here, we fit only four calculated points at each value of $\hbar\Omega$ in the range $N_{\max} = 6-12$, representative of the limited results that we expect to encounter in slightly heavier systems. We select the values of $\hbar\Omega$ to include in the analysis by first taking the value at which the minimum (with respect to $\hbar\Omega$) occurs along the highest $N_{\max}$ curve included in the fit, then taking one $\hbar\Omega$ value lower by 2.5 MeV and three $\hbar\Omega$ values higher by successive increments of 2.5 MeV. Because the minimum occurs along the $N_{\max} = 12$ curve at $\hbar\Omega = 12.5$ MeV as shown in Fig. 6, this produces the five curves spanning a range of 10 MeV in $\hbar\Omega$ shown in Fig. 7. We perform a linear regression for each sequence of four points at fixed $\hbar\Omega$ using an independent exponential plus constant for each sequence and observe a small spread in the extrapolants as is evident in Fig. 7, which is indicative of the uncertainty in this method.

We recognize that this window of results in $\hbar\Omega$ values is arbitrary. Our only assurance is that it seems to provide a consistent set of extrapolations in the nuclei examined in the present work.

For the global extrapolation we chose sets of four points due to a desire to minimize the fluctuations arising from certain "odd-even" effects already visible in Fig. 4. These effects are most pronounced in weakly bound systems and may be attributed to the fact that HO wave functions fall off too fast: wavefunctions of finite nuclei decrease exponentially at large distances. To mimic such an exponential decrease with HO basis functions, one needs HO basis functions with both even principle quantum number n (even number or nodes in radial wave function) and with odd principle quantum number n (odd number or nodes in radial wave function). Because $N = (2n + l)$, a set of four successive $N_{\max}$ points (with $N_{\max}$ even) implies we incorporate two highest allowed HO single-particle states with even values of the principal quantum number and two highest allowed with odd values. Thus, a set of four consecutive $N_{\max}$ points instead of three points (the minimal number of points for an exponential extrapolation) averages out some of these "odd-even" effects. We will come back to this point when we discuss the extrapolation method B, using sets of three points at fixed $\hbar\Omega$.

Next, we consider what weight to assign to each calculated $(N_{\max}, \hbar\Omega)$ point. The fits in Fig. 7 are obtained with equal weights for each of the points. However, as $N_{\max}$ increases, we are approaching the exact result from above with increasing precision. Hence, the importance of results grows with increasing $N_{\max}$ and this should be reflected in the weights assigned to the calculated points used in the fitting procedure. With this in mind, we adopt the following strategy: define a χ^2 function to be minimized and assign a $\sigma_{N_{\max}}$ to the ground-state energy at each $N_{\max}$ value that is the change in the calculated energy from the next lower $N_{\max}$ value

$$\sigma_{N_{\max}} = E_{\rm gs}(N_{\max}) - E_{\rm gs}(N_{\max} - 2).$$

To complete these σ assignments, the σ for the lowest $N_{\max}$ point on the $N_{\max}$ curve is assigned a value three times the sigma calculated for the second point on the same fixed-$\hbar\Omega$ trajectory. As a final element to our global extrapolation strategy, we invoke the minimization principle to argue that all curves of results at fixed $\hbar\Omega$ will approach the same exact answer from above. Thus all curves will have a common asymptote and we use that condition as a constraint on the χ^2 minimization.

When we use exponential fits constrained to have a common asymptote and weights based on the local slope, we obtain curves close to those in Fig. 7. The differences are difficult to perceive in a graph so we omit presenting a separate figure for them in this case. It is noteworthy that the equal weighting of the linear regression leads to a spread in the extrapolants that is still modest.

The sequence of asymptotes for the ^{2}H ground-state energy, obtained with the global extrapolation, by using successive sets of four points in $N_{\max}$ and performing our constrained fits to each such set of four points, is shown in Fig. 8 as extrapolation A. We employ the independent fits such as those in Fig. 7 to define the uncertainty in our asymptotes. In particular, we define our uncertainty, or estimate of the standard deviation for the constrained asymptote, as one-half the total spread in the asymptotes arising from the independent fits with equal weights for each point. On rare occasions, we obtain an outlier when the linear regression produces a residual less than 0.999 that we discard from the determination of the total spread. Also, on rare occasions, the calculated upper uncertainty reaches above the calculated upper bound. When this happens, we reduce the upper uncertainty to the upper bound as it is a strict limit.

One may worry that the resulting extrapolation tool contains several arbitrary aspects and we agree with that concern. One recourse is to cross-check these choices with the solvable NCFC cases in the present subsection and following subsections. We seek consistency of the constrained extrapolations as gauged by the uncertainties estimated from the unconstrained

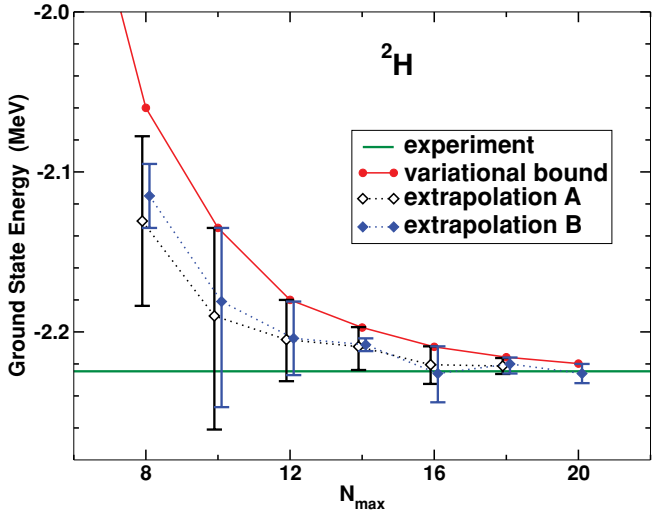

FIG. 8. (Color online) Extrapolated ground-state energies and variational upper bounds from each set of four (extrapolation A) or three (extrapolation B) successive $N_{\max}$ values as a function of the largest value of $N_{\max}$ in each set. Error bars are dominated by the uncertainties in the extrapolations and are obtained as described in the text. Note the expanded scale and the reasonable consistency of the extrapolated results: for $N_{\max} \geqslant 10$ all but one are within their uncertainty range of the exact answer.

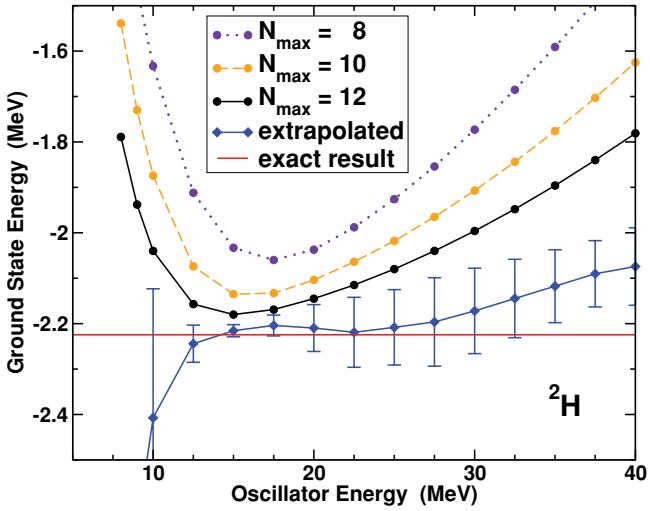

FIG. 9. (Color online) Calculated ground-state energy of ^{2}H for $N_{\max} = 8, 10, 12$, and the extrapolated ground-state energy using method B, as function of the oscillator energy, $\hbar\Omega$. Error bars are obtained from the difference with the extrapolation using $N_{\max} = 6, 8$, and 10 calculations.

extrapolations described above. Indeed, our results, such as those shown in Fig. 8, demonstrate that consistency. The deviation of any specific constrained extrapolant from the result at the highest upper limit $N_{\max}$ appears well characterized by the assigned uncertainty.

2. *Extrapolation at fixed $\hbar\Omega$*

In addition, we also employ an extrapolation at fixed values of $\hbar\Omega$ using only three successive values of $N_{\max}$, the minimal number of points for such an extrapolation (referred to as extrapolation B). Under the assumption that the convergence is indeed exponential, such an extrapolation should get more accurate as $N_{\max}$ increases; the difference between the extrapolated results from two consecutive sets of three $N_{\max}$ values is used here as our estimate of the numerical uncertainty associated with the extrapolation.

In Fig. 9 we illustrate this extrapolation for ^{2}H based on calculations with $N_{\max} = 8, 10$, and 12. As we can see, this extrapolation gives $\hbar\Omega$-dependent results. We therefore consider the value of $\hbar\Omega$ where the extrapolation is most stable (i.e., for which the difference between the extrapolated value and the result at the highest $N_{\max}$ is minimal) as the best or most reliable $\hbar\Omega$ for this extrapolation method. This $\hbar\Omega$ value is usually at or slightly above the variational minimum.

Because this extrapolation uses sets with only three $N_{\max}$ points, the "odd-even" effects may be significant, in particular for weakly bound nuclei. This is indeed what we find for ^{2}H as seen in Fig. 8. Nevertheless, within the estimated error bars, the results are consistent with extrapolation method A and with the exact result. In addition, as we proceed to applications in heavier nuclei and more deeply bound nuclei, this extrapolation becomes more stable and useful, as we will see below.

C. More NCFC test cases: $A = 3, 4$

The ground-state energies of ^{3}H using JISP16 are shown in Fig. 10 as a function of the HO energy for the same sequence of basis spaces as for ^{2}H. We again observe a converging sequence of upper bounds with an indication of a small amount of underbinding compared with experiment. We note that the curves show a greater region of approximate independence of $\hbar\Omega$ than found in the case of ^{2}H as may be expected from the

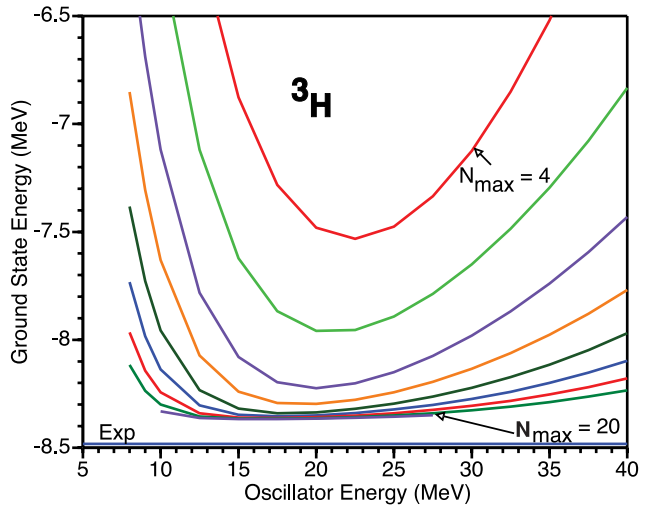

FIG. 10. (Color online) Calculated ground-state energy of ^{3}H as a function of the oscillator energy, $\hbar\Omega$, for selected values of $N_{\max}$. The curve closest to experiment corresponds to the value $N_{\max} = 20$ and successively higher curves are obtained with $N_{\max}$ decreased by two units for each curve.

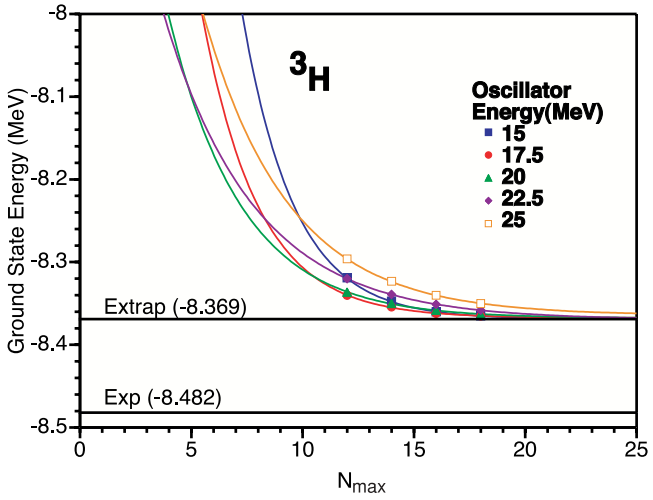

FIG. 11. (Color online) Calculated ground-state energy of ^{3}H as a function of N_{max} at $\hbar\Omega$ values that bracket the best upper bound. The smooth curves are fits of an exponential plus a constant [see Eq. (1)] to the four data points shown at each value of $\hbar\Omega$. There is a 5-keV spread in these asymptotes that is used to assign the uncertainty to the asymptote derived from the constrained fit as described in the text. The asymptote of the constrained global fit (extrapolation A) is quoted in the figure and the experimental result is shown for comparison.

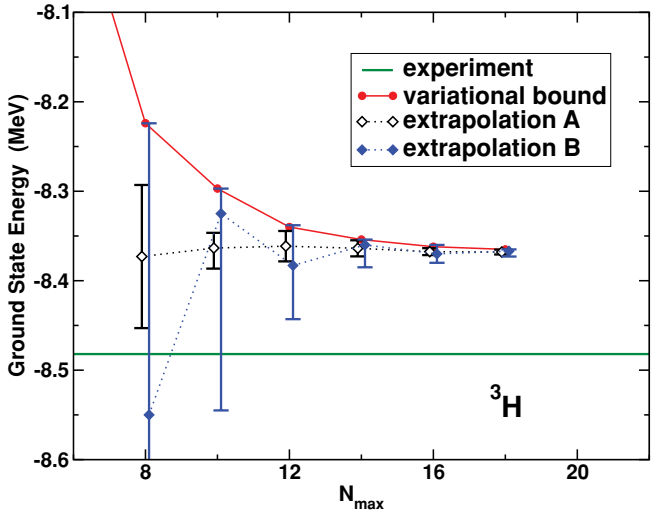

FIG. 12. (Color online) Extrapolated ground-state energies and variational upper bounds from each set of four (extrapolation A) or three (extrapolation B) successive N_{max} values as a function of the largest value of N_{max} in each set. Error bars are dominated by the uncertainties in the extrapolations and obtained as described in the text. Note the consistency of the extrapolated results.

stronger binding relative to the first breakup threshold in the present situation.

We use the case of ^{3}H to illustrate again the utility of the global extrapolation (A). Results of independent fits with equal weights for each calculated point are shown in Fig. 11 to demonstrate the nearly identical asymptote when results are available at sufficiently high N_{max} values. We depict in Fig. 11 both the experimental value and the asymptote of the global extrapolation using the four-point sequence up to $N_{max} = 18$. The span of $\hbar\Omega$ values is selected in the same manner as in the ^{2}H case, the procedure we will use throughout this work.

As for the case of ^{2}H, we also present the sequence of extrapolated results for the ^{3}H ground-state energy in Fig. 12 using both extrapolation methods A and B, together with the variational bound. Both extrapolation methods appear to be consistent with each other and give numerical error bars that decrease with increasing N_{max}. The extrapolation B, using only three successive N_{max} points at fixed $\hbar\Omega$, shows a rather strong "odd-even" effect. Nevertheless, all extrapolated results agree, within error bars, with each other, and with our best results at $N_{max} = 18$. These results are also quoted in Table I. We conclude that JISP16 underbinds ^{3}H by approximately 113 keV.

Our calculations for ^{3}He show a similar convergence pattern as those for ^{3}H. At $N_{max} = 18$, our results are within a few keV of full convergence, as can be seen from Table I, and we find JISP16 underbinds ^{3}He by about 52 keV.

As a final test of our extrapolations we consider ^{4}He. We present our calculations as a function of $\hbar\Omega$ at fixed values of N_{max} in Fig. 13. The results clearly indicate rapid convergence in both N_{max} and $\hbar\Omega$; at $N_{max} = 16$ the ground-state energy is converged to within 1 keV over the range 20 MeV $\leqslant \hbar\Omega \leqslant$ 25 MeV. Furthermore, the fully converged NCFC ground-state energy is within 3 keV of the experimental energy as shown in Table I. As illustrations of our extrapolations, we demonstrate in Fig. 14 the independent fits used to assess uncertainties of extrapolation A based on $N_{max} = 2$ to $N_{max} = 8$ results. In addition, Fig. 15 shows extrapolation B at fixed values of $\hbar\Omega$ using $N_{max} = 8$, 10, and 12 results.

We also confirm that the dependence on N_{max} at fixed $\hbar\Omega$ is nearly a pure exponential as illustrated best in Fig. 16 where we show a wider range of the calculated results. Here, we

TABLE I. Binding energies in MeV of nine nuclei and of the first excited 0^+ states in ^{12}C and ^{16}O from experiment and theory. The experimental values are from Refs. [19–24]. The uncertainties in the rightmost digits of an extrapolation are quoted in parenthesis. The bounds for the binding energies follow from the variational upper bounds for the ground-state energies. The rightmost column provides the uppermost value of N_{max} used in the quoted extrapolations.

Nucleus (J^P)	Exp.	Extrap. A	Extrap. B	Variational bound	Max N_{max}
^{2}H (1^+)	2.225	2.223(5)	2.226(6)	2.220	20
^{3}H ($\frac{1}{2}^+$)	8.482	8.369(1)	8.3695(25)	8.367	18
^{3}He ($\frac{1}{2}^+$)	7.718	7.665(1)	7.668(5)	7.663	18
^{4}He (0^+)	28.296	28.299(1)	28.299(1)	28.298	16
^{6}He (0^+)	29.269	28.68(12)	28.69(5)	28.473	14
^{6}Li (1^+)	31.995	31.43(12)	31.45(5)	31.185	14
^{8}He (0^+)	31.408	29.74(34)	30.05(60)	28.927	12
^{12}C (0^+_1)	92.162	93.9(1.1)	95.1(2.7)	90.9	8
^{12}C (0^+_2)	84.508	80.7(2.3)	–	–	8
^{16}O (0^+_1)	127.619	143.5(1.0)	150(14)	134.5	8
^{16}O (0^+_2)	121.570	130.6(7.6)	–	–	8

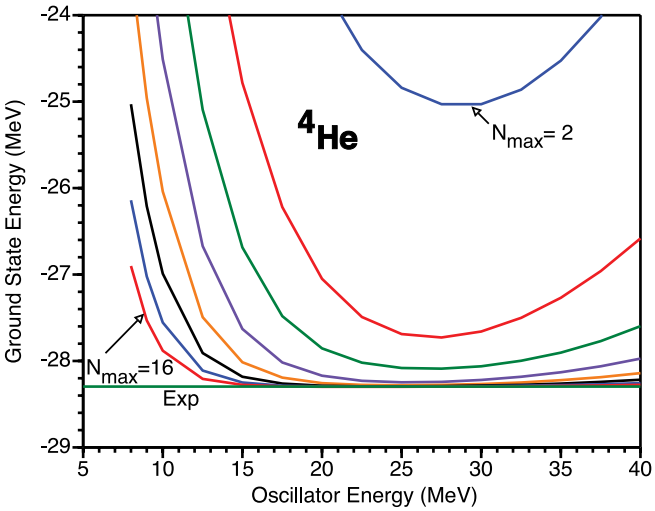

FIG. 13. (Color online) Calculated ground-state energy of ^{4}He as function of the oscillator energy, $\hbar\Omega$, for a sequence of $N_{\max}$ values. The curve closest to experiment corresponds to the value $N_{\max} = 16$ and successively higher curves are obtained with $N_{\max}$ decreased by 2 units for each curve.

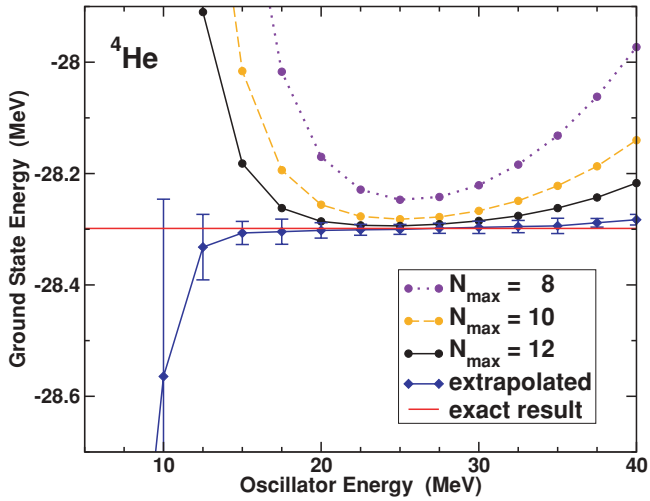

FIG. 15. (Color online) Calculated ground-state energy of ^{4}He for $N_{\max} = 8$, 10, 12, and the extrapolated ground-state energy using method B, as function of the oscillator energy, $\hbar\Omega$. Error bars are obtained from the difference with the extrapolation using $N_{\max} = 6$, 8, and 10 calculations.

provide regression analyses for each set of results spanning $N_{\max} = 2-16$ at fixed $\hbar\Omega$ values ranging from 15 to 35 MeV. For both basis space parameters, this is a significantly wider range of parameter values than we use in our applications below.

We present the NCFC results of both extrapolation methods in Fig. 17 along with the experimental and variational upper bound energies. In this case the results produce very rapid convergence with uncertainties that drop precipitously with increasing $N_{\max}$ as seen in the figure. We note that the error bars conservatively represent the extrapolation uncertainties because all the extrapolated results are, within their error bars, consistent with each other and with the fully converged NCFC result. The largest $N_{\max}$ points define the results quoted in Table I, a ground-state overbound by 3 ± 1 keV.

We have seen in this section that the NCFC results for three light nuclei provide sufficiently converged ground-state energies to allow us to test our extrapolation methods and confirm the validity of their assigned uncertainties. In what follows, we present NCFC calculations for five nuclei using both extrapolations A and B. The five nuclei selected for this initial application consist of stable and unstable even nuclei that span the p shell. We include two loosely bound nuclei,

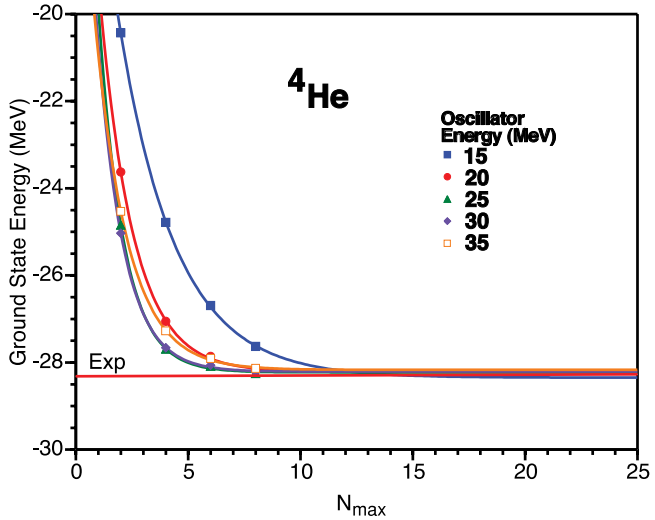

FIG. 14. (Color online) Calculated ground-state energy of ^{4}He for $N_{\max} = 2-8$ at selected values of $\hbar\Omega$. Each set of four points is fit, using equal weights, with an exponential plus constant [see Eq. (1)] producing the solid curves. Half the resulting spread in the asymptotic values is used to determine the uncertainty assigned to the first point in Fig. 17 for extrapolation A as described in the text.

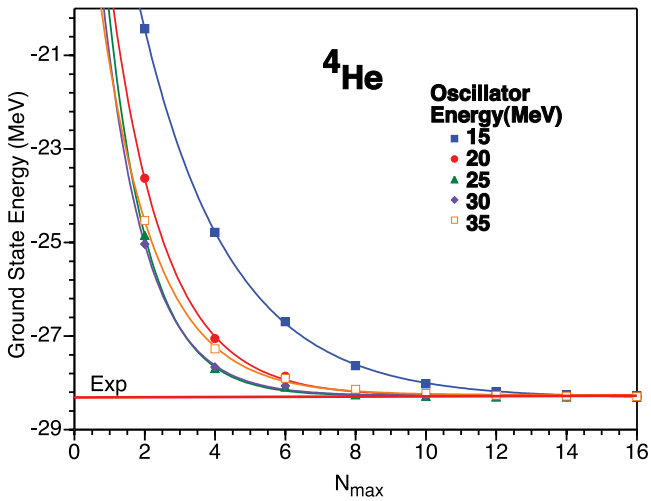

FIG. 16. (Color online) Calculated ground-state energy of ^{4}He for $N_{\max} = 2-16$ for JISP16 at selected values of $\hbar\Omega$. Each set of eight points at fixed $\hbar\Omega$ is fit by Eq. (1) producing the solid curves. Each point is a true upper bound to the exact answer. The asymptotes $E_{\rm gs}(\infty)$ are the same to within 35 keV of their average value and they span the experimental ground-state energy.

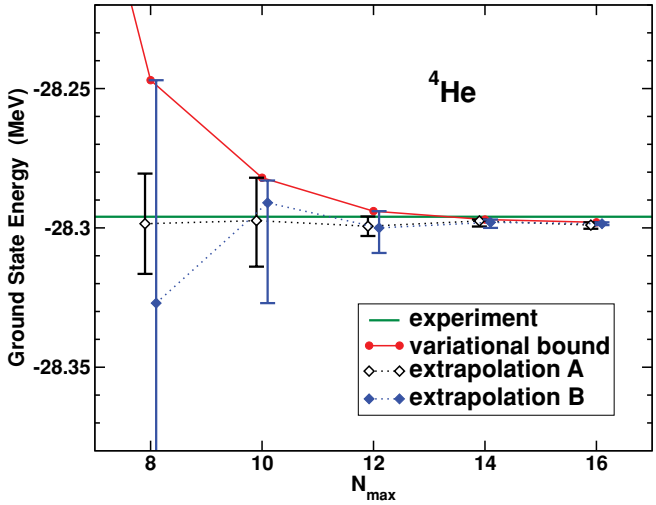

FIG. 17. (Color online) Extrapolated ground-state energies and variational upper bounds from each set of four (extrapolation A) or three (extrapolation B) successive $N_{\max}$ values as a function of the largest value of $N_{\max}$ in each set. Error bars represent the assessed uncertainties in the extrapolations and are obtained as described in the text. Note the consistency of the extrapolations: the exact answer is well within the uncertainty range of the extrapolations for all $N_{\max}$ points, with the uncertainty diminishing with increasing $N_{\max}$.

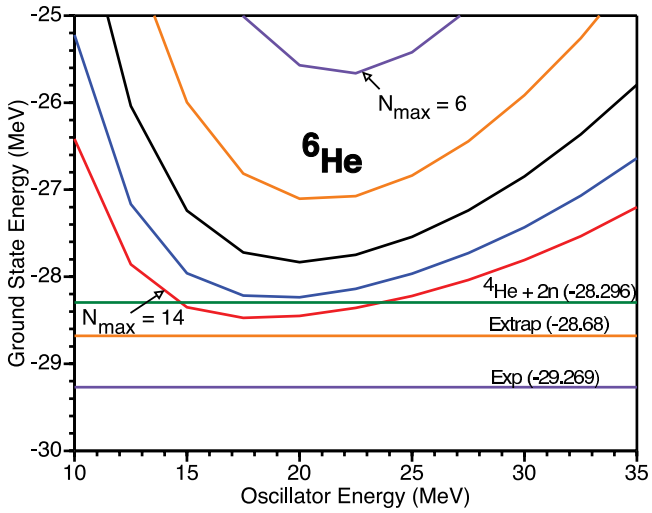

FIG. 18. (Color online) Calculated ground-state energy of ^{6}He as function of the oscillator energy, $\hbar\Omega$, for selected values of $N_{\max}$. The figure displays also the experimental result, the common asymptote from the global extrapolation (A), and the experimental threshold for the $\alpha + 2n$ breakup. The curve closest to experiment corresponds to the value $N_{\max} = 14$ and successively higher curves are obtained with $N_{\max}$ decreased by two units for each curve.

^{6}He and ^{8}He, anticipating that they will provide challenges for achieving a converged ground-state energy.

D. NCFC results for ^{6}He, ^{6}Li, and ^{8}He

By comparing Figs. 6, 10, and 13 we observe clearly the marked correlation between binding energy and convergence rate—the more deeply bound ground states exhibit greater independence of $\hbar\Omega$ at fixed $N_{\max}$. A more complete picture of this correlation is seen below, for example, with the ^{6}He and ^{6}Li results where one observes that the relevant energy scale governing the rate of convergence is the binding with respect to the nearest threshold. Our physical intuition supports this correlation because we know the asymptotic tails of the bound-state wave functions fall more slowly as one approaches a threshold for dissociation. This same intuition tells us to expect Coulomb barriers and angular momenta to play significant roles in this correlation.

Consider first the weakly bound nucleus ^{6}He presented in Figs. 18, 19, and 20. In the largest basis spaces achieved, $N_{\max} = 14$, we obtain net binding with respect to the breakup threshold as seen in Fig. 18. However, the results appear farther from convergence than the case for ^{4}He in the same $N_{\max}$ spaces depicted in Fig. 13. Note the proximity of the $^4\text{He} + 2n$ breakup threshold to the calculated ground-state energies that suggests the importance of achieving results at $N_{\max} = 16$ as well as obtaining improved nuclear Hamiltonians that better reproduce the experimental binding of ^{6}He.

To examine this situation in some detail, we present in Fig. 19 results as a function of $N_{\max}$ that covers a range of 15 MeV in $\hbar\Omega$ values. We also present the linear regression analyses for the range of $N_{\max} = 2-14$ to show that the exponential fit appears to maintain its validity. Thus, we proceed with the extrapolation methods as developed and tested in previous sections and display the results in Fig. 20.

Because we use only three $N_{\max}$ points for our extrapolation B, at fixed values of $\hbar\Omega$, we also include extrapolated results based on $N_{\max} = 2$, 4, and 6; with an error

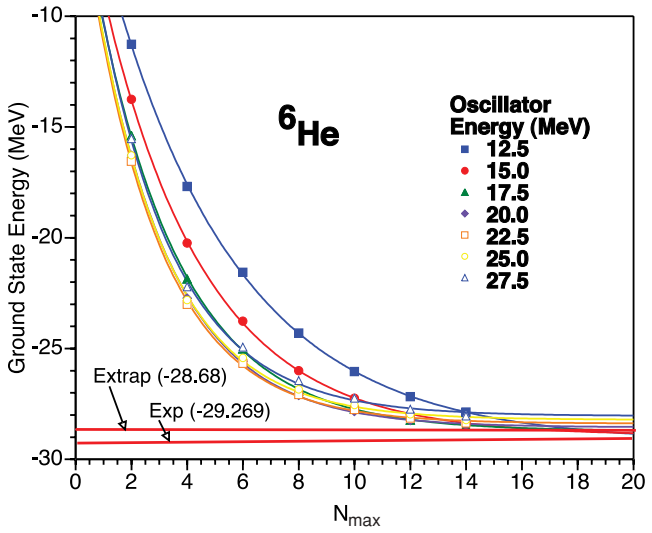

FIG. 19. (Color online) Calculated ground-state energy of ^{6}He for $N_{\max} = 2-14$ for JISP16 at selected values of $\hbar\Omega$. Each set of points at fixed $\hbar\Omega$ is fit by Eq. (1) using equal weights producing the solid curves. Each point is a true upper bound to the exact answer. The resulting asymptotes $E_{\text{gs}}(\infty)$ are the same to within 600 keV of their average value. The figure displays the experimental result and the common asymptote from the global extrapolation (A) as described in the text.

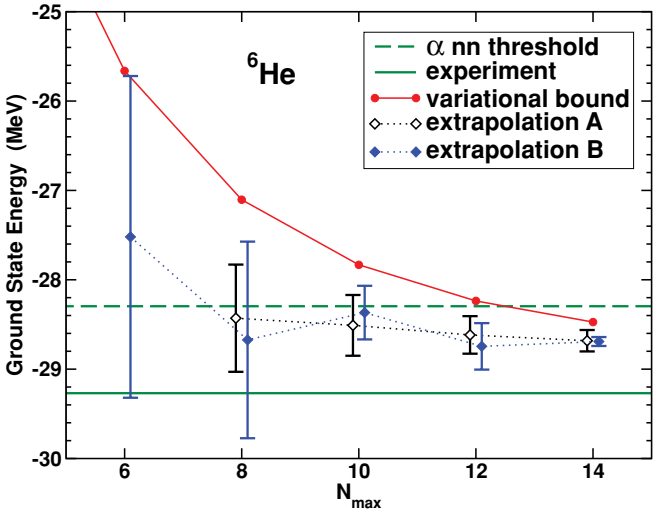

FIG. 20. (Color online) Extrapolated ground-state energies and upper bounds from sets of successive N_{max} values as a function of the largest value of N_{max} in each set. Uncertainties are determined for each value of $\hbar\Omega$ as described in the text. Note the consistency of the extrapolated results as they fall well within their uncertainty ranges along the paths of converging sequences.

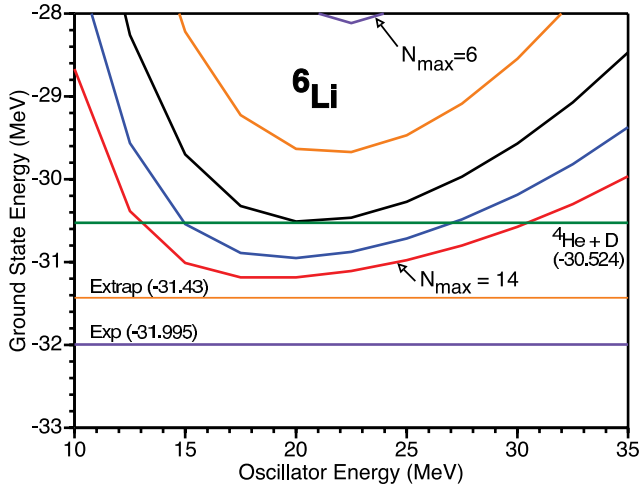

FIG. 21. (Color online) Calculated ground-state energy of ^{6}Li as function of the oscillator energy, $\hbar\Omega$, for selected values of N_{max}. The curve closest to experiment corresponds to the value $N_{max} = 14$ and successively higher curves are obtained with N_{max} decreased by two units for each curve. The figure displays also the global extrapolation (A) and the threshold for the $\alpha + d$ breakup.

estimated based on the difference between the $N_{max} = 6$ calculation and the extrapolated result. Such an extrapolation, based on a rather small model space, can be useful for larger nuclei, and it turns out to be quite reasonable. However, we do see a rather significant "odd-even" effect with extrapolation B for this nucleus.

The results from the highest value of the upper limit in N_{max} are provided in Table I. We again observe consistency in the results the the global and fixed $\hbar\Omega$ extrapolations. The JISP16 interaction yields about 600 keV underbinding in ^{6}He that implies the theoretical proton rms radius will likely be too large compared with experiment.

Next, we turn our attention to ^{6}Li and present our NCFC results using extrapolations in Figs. 21, 22, and 23. As in the ^{6}He case, there is a low-lying threshold for breakup—here about 1.47 MeV above the experimental ground state. Both our $N_{max} = 12$ and 14 curves drop below this threshold over a range of $\hbar\Omega$ values as seen in Fig. 21.

Our global extrapolation for ^{6}Li is depicted in Fig. 22 where we select the case with the highest upper limit in N_{max} to portray. The minimum in $\hbar\Omega$ at $N_{max} = 14$ occurs at $\hbar\Omega = 20$ MeV. According to our global extrapolation, we then perform the constrained fit on the results in the span $\hbar\Omega = 17.5-27.5$ MeV in 2.5-MeV increments to obtain the fits shown in Fig. 22. The asymptote, the extrapolant (−31.43 MeV), becomes the last data point on the right in Fig. 23 where the uncertainty is obtained in the manner described above. We also perform our extrapolation at fixed values of $\hbar\Omega$ and find results consistent with our global extrapolation; see Fig. 23.

The extrapolated results are entered in Table I and compared with experiment. We find that ^{6}Li is underbound by about 560 keV with the JISP16 interaction, similar to the amount of underbinging for ^{6}He; the rate of convergence and error estimate in our final answer are also similar. However, the "odd-even" effect we found with extrapolation B for the other nuclei (including ^{8}He below) is absent in ^{6}Li.

Next, let us consider another weakly bound nucleus, ^{8}He. In Fig. 24 we show our results for the ^{8}He ground-state energy as function of $\hbar\Omega$ for several values of N_{max}, together with the extrapolated results at fixed $\hbar\Omega$ and our result from the global extrapolation. The extrapolated energies and their uncertainties are presented in Fig. 25 as function of N_{max}, together with the variational upper bounds. For comparison, we also show the experimental value, and the thresholds for $\alpha + 4n$ breakup and for ^{6}He + $2n$ breakup.

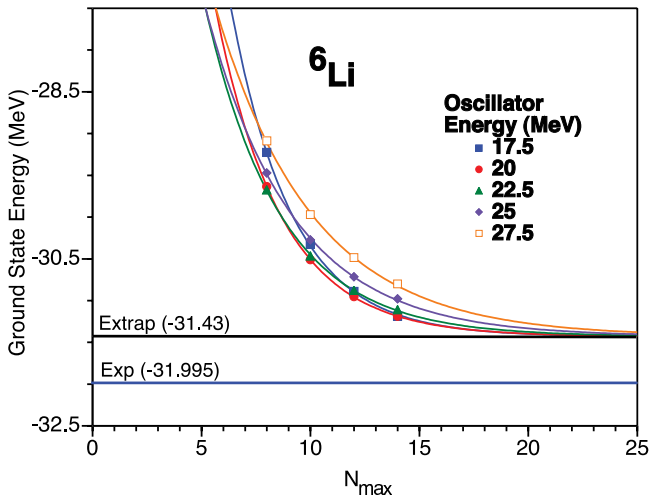

FIG. 22. (Color online) Calculated ground-state energy of ^{6}Li for $N_{max} = 8-14$ at values of $\hbar\Omega$ that span the minimum at $N_{max} = 14$. Curves define the fits using the global extrapolation (A) that produces a common constant, the asymptote, labeled by "Extrap".

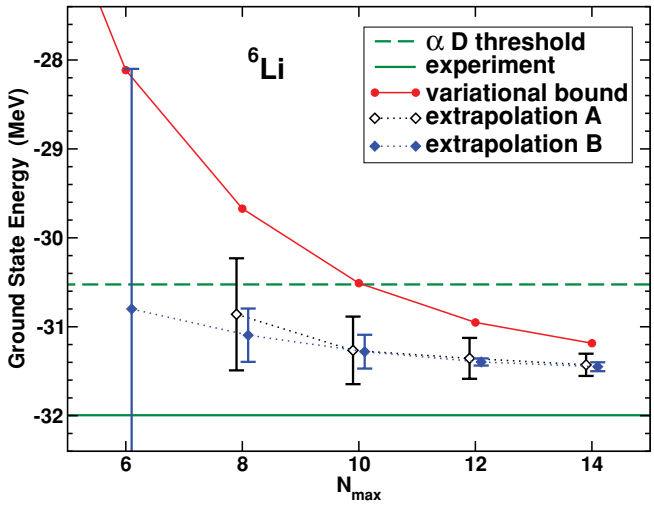

FIG. 23. (Color online) Upper bounds and extracted asymptotes for the ground-state energy of ^{6}Li from each set of successive $N_{\max}$ values as a function of the largest value of $N_{\max}$ in each set. Uncertainties in the asymptotes are determined as described in the text. Note the consistency of the extrapolated results as they fall well within their uncertainty ranges along the paths of converging sequences.

Clearly, the results are not as well converged as those for lighter nuclei, because we are limited to a smaller model space, $N_{\max} = 12$. Nevertheless, the variational upper bound on the ground-state energy is well below the $\alpha + 4n$ threshold. Furthermore, the extrapolations are consistent with each other, and the error bars decrease with increasing $N_{\max}$. Our final NCFC result is not only below the $\alpha + 4n$ threshold but also below the experimental ^{6}He $+ 2n$ breakup threshold, even taking into account the uncertainty in the extrapolation, as can be seen from Fig. 25 and Table I. Compared to the experiment,

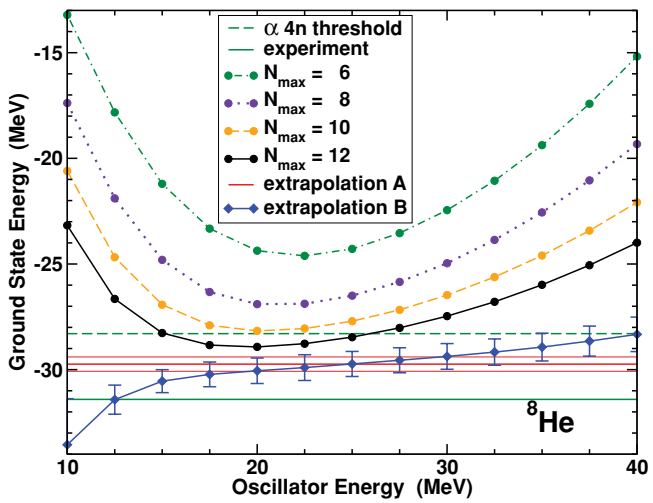

FIG. 24. (Color online) Calculated ground-state energy of ^{4}He for $N_{\max} = 6, 8, 10, 12$, and the extrapolated ground-state energies using method B, as well as the result from extrapolation method A, with error bars. For comparison, we also show the experimental value, and the threshold for $\alpha + 4n$ breakup.

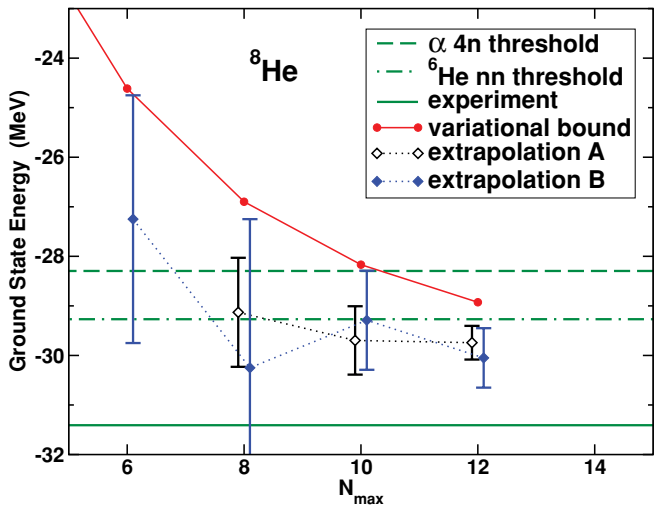

FIG. 25. (Color online) Upper bounds and extrapolated ground-state energies of ^{8}He from each set of successive $N_{\max}$ values as a function of the largest value of $N_{\max}$ in each set. Uncertainties in the asymptotes are determined as described in the text.

we find that ^{8}He is underbound by about 1.6 ± 0.4 MeV with JISP16.

V. NCFC RESULTS FOR ^{12}C AND ^{16}O

Having illustrated the application of our methods with a range of light nuclei, we finally turn to heavier nuclei, and perform NCFC calculations for ^{12}C and ^{16}O. For these nuclei, we can only go to $N_{\max} = 8$, so we have to rely on the extrapolation methods.

A. Extrapolating ^{12}C

The dimension of the model space for ^{12}C with $N_{\max} = 8$ and limited to total $M = 0$ states in the m-scheme is 594,496,743; and the total number of nonzero matrix elements in the lower triangle of the extremely sparse many-body Hamiltonian matrix is 539,731,979,351 with NN interactions only. Thus, storage of one vector in this model space requires 2.4 GB, and storage of the lower triangle of the matrix requires 4.3 TB. The dimension of the $N_{\max} = 10$ basis space is 7,830,355,795, which is beyond our present capabilities.

In Fig. 26 we show our results for ^{12}C for $N_{\max} = 0$ through $N_{\max} = 8$. Because $N_{\max} = 0$ is generally not very reliable for our extrapolations, we have only the extrapolation from the $N_{\max} = 2-8$ results. To illustrate the details of our uncertainties, we depict in Fig. 27 the linear regression analyses of our results spanning the minimum in $\hbar\Omega$ obtained at $N_{\max} = 8$. Our global extrapolation A produces a ground-state energy of 93.9 ± 1.1 MeV, whereas the extrapolation B at fixed $\hbar\Omega = 27.5$ MeV (where it is most stable) gives 95.1 ± 2.7 MeV. Given the "odd-even" effect that often plagues extrapolation B, in combination with the smaller error bar obtained with extrapolation A, we conclude that JISP16 produces a binding energy of about 94 MeV with an

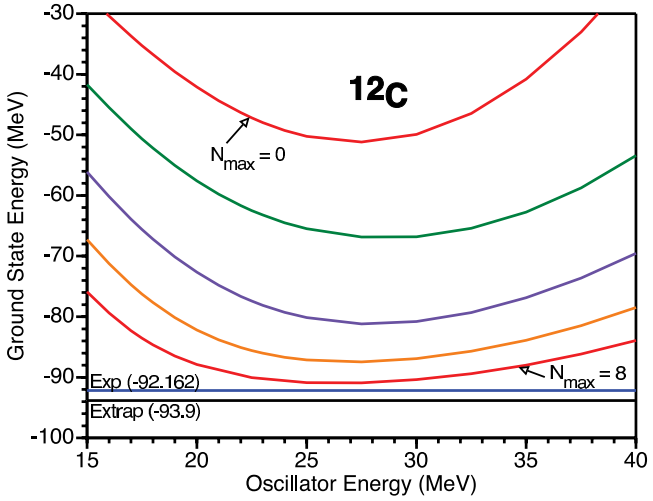

FIG. 26. (Color online) Calculated ground-state energy of ^{12}C as function of the oscillator energy, $\hbar\Omega$, for selected values of $N_{\max}$. The curve closest to experiment corresponds to the value $N_{\max} = 8$ and successively higher curves are obtained with $N_{\max}$ decreased by 2 units for each curve.

uncertainty of 1% to 2%; or in other words, it overbinds ^{12}C by about 1.8 MeV.

For a speculative application, we also consider the first excited 0^+ state of ^{12}C, the "Hoyle state" or "triple alpha" state as it has come to be known. Because experimentally, this state, with $E_{\text{Hoyle}} = -84.51$ MeV, is just above the threshold for breakup into three α's, $3\,E_\alpha = -84.89$ MeV, it may be poorly converged. However, our calculations for both ^{6}He and ^{8}He at $N_{\max} = 2-8$ are above breakup into α plus neutrons, but the extrapolations from these points produce results with error bars of about 1 MeV and agree with our best calculations

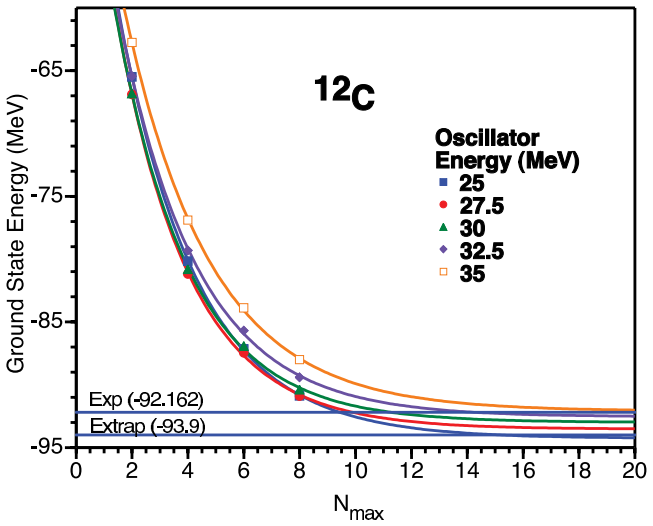

FIG. 27. (Color online) Calculated ground-state energy of ^{12}C for $N_{\max} = 2-8$ at selected values of $\hbar\Omega$ as described in the text. For each $\hbar\Omega$ the data are fit by Eq. (1). These independent asymptotes $E_{\text{gs}}(\infty)$ provide a measure of our uncertainty within the global extrapolation (A). The figure displays the experimental ground-state energy and the common asymptote obtained in the global extrapolation.

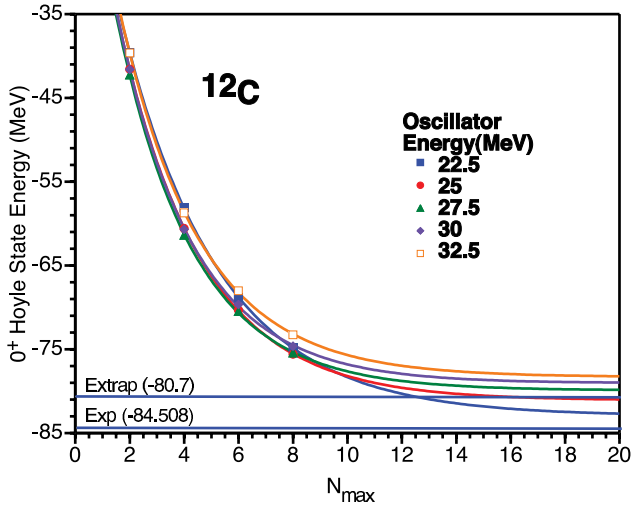

FIG. 28. (Color online) Calculated energy of ^{12}C first excited 0^+ state (Hoyle state) for $N_{\max} = 2-8$ at selected values of $\hbar\Omega$ as described in the text. For each $\hbar\Omega$ the data are fit by Eq. (1). These independent asymptotes $E_{\text{gs}}(\infty)$ provide a measure of our uncertainty within the global extrapolation (A). The figure displays the experimental energy and the common asymptote of the global extrapolation.

at $N_{\max} = 12$. Encouraged by these results for ^{6}He and ^{8}He at $N_{\max} = 8$, we apply the global extrapolation method A to the first excited 0^+ state of ^{12}C. The calculated results and extrapolation are shown in Fig. 28 and summarized in Table I. Our extrapolation gives $E_{\text{Hoyle}} = -80.7 \pm 2.3$ MeV, corresponding to an excitation energy of 13 ± 3 MeV, compared to an experimental excitation energy of 7.654 MeV. It remains to be seen how reliable the extrapolation is for this (and similar) states. One may even expect this extrapolation to be unreliable as solutions obtained in our present, very limited, basis spaces may not accommodate all the essential physics of such excited states. Nevertheless, assuming that our error estimates are realistic, our conclusion is that JISP16 overbinds the ground state of ^{12}C by an MeV or two, but underbinds the first excited 0^+ state by about 2 to 6 MeV. When combined, that means it produces an excitation energy that is significantly too large.

B. Extrapolating ^{16}O

Finally, we consider ^{16}O with $N_{\max} = 8$. The dimension of the corresponding model space is 996,878,170; and the total number of nonzero matrix elements in the lower triangle of the many-body matrix is 805,811,591,748 with NN interactions only. Thus, storage of one vector in this model space requires 4.0 GB, and storage of the lower triangle of the matrix requires 6.5 TB.

The results for ^{16}O are shown in Figs. 29 and 30, and summarized in Table I. As in the case of ^{12}C, we only attain the results through $N_{\max} = 8$ with our current capabilities. Thus, we have a single extrapolant using $N_{\max} = 2$, 4, 6, and 8 (extrapolation A) or use extrapolation B for $N_{\max} = 4$, 6, and 8. The extrapolation B gives a lower estimated ground-state

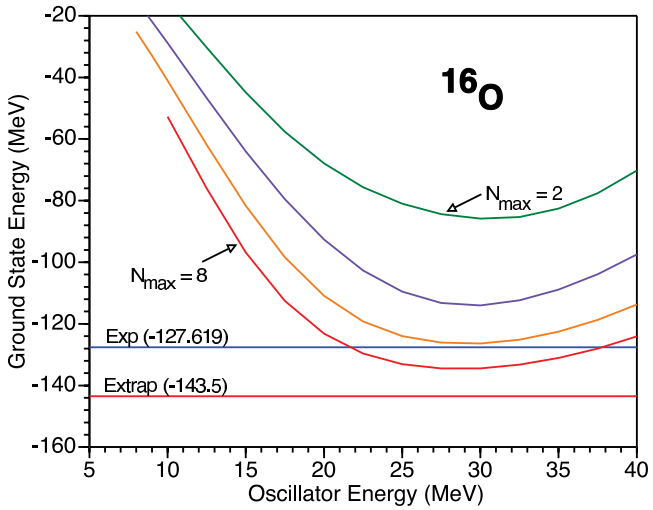

FIG. 29. (Color online) Calculated ground-state energy of ^{16}O as function of the oscillator energy, $\hbar\Omega$, for selected values of $N_{\max}$. The curve closest to experiment corresponds to the value $N_{\max} = 8$ and successively higher curves are obtained with $N_{\max}$ decreased by 2 units for each curve.

energy with a significantly larger uncertainty (10%) compared to extrapolation A. We anticipate that this difference is due to the "odd-even" effect we have seen in most light nuclei using extrapolation B and expect that the results obtained with extrapolation A are more realistic for this case. Also note that the variational upper bound on the ground-state energy is below the experimental ground state. That implies that JISP16 produces an overbinding of at least 7 MeV and more likely about 15 to 18 MeV for ^{16}O.

For another speculative application, we also consider the first excited 0^+ state of ^{16}O, believed to have a significant cluster structure. Experimentally, this state is very close to

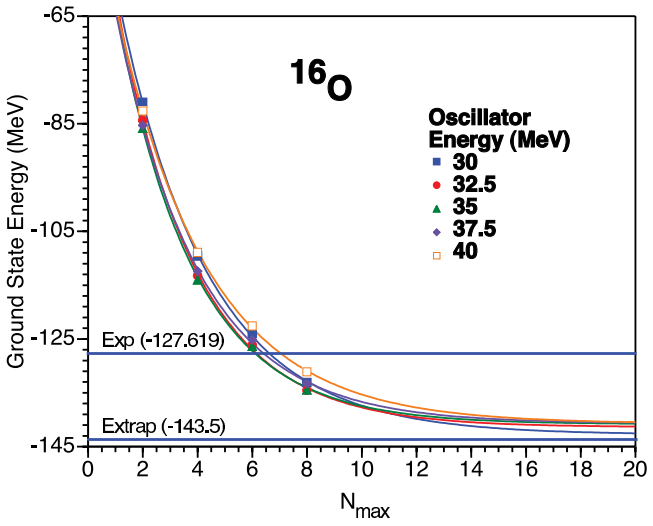

FIG. 30. (Color online) Calculated ground-state energy of ^{16}O for $N_{\max} = 2-8$ at selected values of $\hbar\Omega$ as described in the text. For each $\hbar\Omega$, the data are fit to an exponential plus a constant, the asymptote. The figure displays the experimental ground-state energy and the common asymptote obtained in the global extrapolation (A).

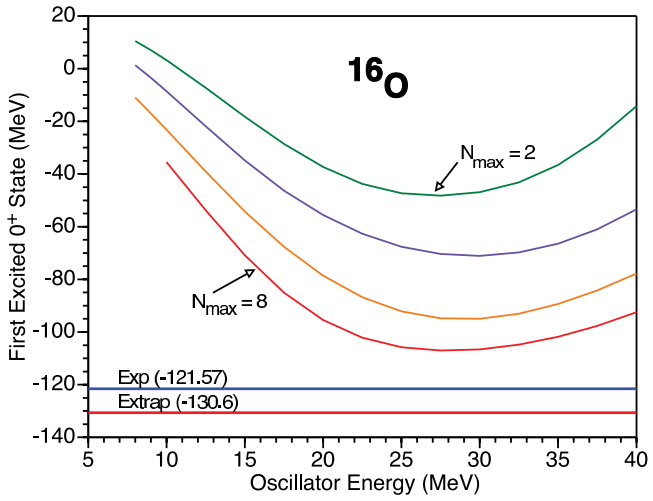

FIG. 31. (Color online) Calculated first excited 0^+ state energy of ^{16}O as function of the oscillator energy, $\hbar\Omega$, for selected values of $N_{\max}$. The curve closest to experiment corresponds to the value $N_{\max} = 8$ and successively higher curves are obtained with $N_{\max}$ decreased by 2 units for each curve. The figure displays the experimental excited state energy and the common asymptote obtained in the global extrapolation (A).

threshold for breakup into ^{12}C plus an α particle. Applying extrapolation A, we find $E_{\text{excited}} = -130.6 \pm 7.6$ MeV, showing an even larger extrapolation uncertainty than for the Hoyle state in ^{12}C. Compared to experiment, we find an excitation energy of 13 ± 8 MeV compared to 6.05 MeV experimentally. Given the large uncertainty in the extrapolation for this state, we cannot draw any conclusions without results in larger model spaces regarding this excited state.

VI. CONCLUSIONS AND OUTLOOK

We present in Table I a summary of our results, using extrapolations, performed with methods introduced here and compare them with the experimental results. In all cases, we used the calculated results to the highest $N_{\max}$ available with the bare JISP16 interaction. In the cases of the lightest nuclei, the extrapolations were rather modest as nearly converged results were obtained directly. The uncertainties apply to the least significant digits quoted in the table.

Our overall conclusion is that these results demonstrate sufficient convergence is achieved for ground-state energies of light nuclei to allow extrapolations to the infinite basis limit and to estimate their uncertainties. Thus, we have achieve *ab initio* NCFC results for these nuclei with our chosen Hamiltonian.

The convergence rate reflects the short-range properties of the nuclear Hamiltonian. Fortunately, new renormalization schemes have been developed and applied that show promise for providing suitable nuclear Hamiltonians with good convergence properties [25]. Additional work is needed to develop the corresponding NNN interaction. Also, further work is in progress to develop extrapolation tools for the rms radii. Of course, the rms radii present a greater challenge because they are more sensitive than the energies to the asymptotic properties of the wave functions.

ACKNOWLEDGMENTS

We thank Miles Aronnax for calculating some of the dimensions plotted in Fig. 1. We thank Petr Navrátil for the chiral N3LO results shown in Fig. 3. We also thank Richard Furnstahl, Petr Navrátil, and Christian Forssen for useful discussions. This work was supported in part by the US Department of Energy Grants DE-FC02-07ER41457 and DE-FG02-87ER40371 and by the Russian Foundation of Basic Research. Results are obtained through Grants of supercomputer time at NERSC and at ORNL. The ORNL resources are obtained under the auspices of an INCITE Grant (David Dean, PI). We especially wish to acknowledge MFDn code improvements [14] developed in Collaboration with Masha Sosonkina (Ames Laboratory), Hung Viet Le (Ames Laboratory), Anurag Sharda (Iowa State University), Esmond Ng (Lawrence Berkeley National Laboratory, LBNL), Chao Yang (LBNL), and Philip Sternberg (LBNL).

[1] S. Weinberg, Physica A **96**, 327 (1979); Phys. Lett. **B251**, 288 (1990); Nucl. Phys. **B363**, 3 (1991).

[2] C. Ordonez, L. Ray, and U. van Kolck, Phys. Rev. Lett. **72**, 1982 (1994); Phys. Rev. C **53**, 2086 (1996).

[3] D. R. Entem and R. Machleidt, Phys. Rev. C **68**, 041001(R) (2003).

[4] P. Navrátil, V. G. Gueorguiev, J. P. Vary, W. E. Ormand, and A. Nogga, Phys. Rev. Lett. **99**, 042501 (2007).

[5] P. Navrátil, J. P. Vary, and B. R. Barrett, Phys. Rev. Lett. **84**, 5728 (2000); Phys. Rev. C **62**, 054311 (2000).

[6] H. Zhan, A. Nogga, B. R. Barrett, J. P. Vary, and P. Navrátil, Phys. Rev. C **69**, 034302 (2004).

[7] C. Forssen, J. P. Vary, E. Caurier, and P. Navrátil, Phys. Rev. C **77**, 024301 (2008).

[8] By "bare," we mean that we have not performed renormalization by means of a Lee-Suzuki-Okamoto or other effective interaction approach.

[9] P. Navrátil (private communication, 2007).

[10] A. M. Shirokov, J. P. Vary, A. I. Mazur, and T. A. Weber, Phys. Lett. **B644**, 33 (2007).

[11] A Fortran program for the JISP16 interaction matrix elements is available at http://nuclear.physics.iastate.edu.

[12] D. H. Gloeckner and R. D. Lawson, Phys. Lett. **B53**, 313 (1974).

[13] J. P. Vary, "The Many-Fermion-Dynamics Shell-Model Code," Iowa State University, 1992 (unpublished); J. P. Vary and D. C. Zheng, *ibid*. 1994 (unpublished); demonstration runs can be performed through, http://nuclear.physics.iastate.edu/mfd.php.

[14] P. Sternberg, E. G. Ng, C. Yang, P. Maris, J. P. Vary, M. Sosonkina, and H. V. Le, in *Proceedings of the 2008 ACM/IEEE Conference on Supercomputing*, Austin, Texas 2008. Conference on High Performance Networking and Computing. IEEE Press, Piscataway, NJ, 1–12, http://doi.acm.org/10.1145/1413370.1413386/.

[15] C. M. Perey and F. G. Perey, Nucl. Data Tables **10**, 540 (1972).

[16] Y. Alhassid, G. F. Bertsch, and L. Fang, Phys. Rev. Lett. **100**, 230401 (2008).

[17] M. Horoi, A. Volya, and V. Zelevinsky, Phys. Rev. Lett. **82**, 2064 (1999); M. Horoi, B. A. Brown, and V. Zelevinsky, Phys. Rev. C **65**, 027303 (2002); **67**, 034303 (2003); M. Horoi, J. Kaiser, and V. Zelevinsky, *ibid*. **67**, 054309 (2003).

[18] A. M. Shirokov, A. I. Mazur, S. A. Zaytsev, J. P. Vary, and T. A. Weber, Phys. Rev. C **70**, 044005 (2004).

[19] F. Ajzenberg-Selove, Nucl. Phys. **490**, 1 (1988).

[20] Y. Fujita *et al*., Phys. Rev. C **70**, 011306(R) (2004).

[21] F. Ajzenberg-Selove, Nucl. Phys. **A506**, 1 (1990).

[22] I. Tanihata, T. Kobayashi, O. Yamakawa, S. Shimoura, K. Ekuni, K. Sugimoto, N. Takahashi, T. Shimoda, and H. Sato, Phys. Lett. **B206**, 592 (1988).

[23] A. Ozawa, I. Tanihata, T. Kobayashi, Y. Sugihara, O. Yamakawa, K. Omata, K. Sugimoto, D. Olson, W. Christie, and H. Wieman, Nucl. Phys. **A608**, 63 (1996); H. De Vries, C. W. De Jager, and C. De Vries, At. Data Nucl. Data Tables **36**, 495 (1987).

[24] F. Ajzenberg-Selove, Nucl. Phys. **A523**, 1 (1991).

[25] S. K. Bogner, R. J. Furnstahl, P. Maris, R. J. Perry, A. Schwenk, and J. P. Vary, Nucl. Phys. **A801**, 21 (2008).